TM-71-1022-5

TECHNICAL MEMORANDUM

STABILITY AND RESPONSE OF THE CMG-CONTROLLED FLEXIBLE SKYLAB

Bellcomm

STABILITY AND RESPONSE OF THE CMG-CONTROLLED FLEXIBLE SKYLAB

Bellcomm, Inc.
Washington, D. C.

Sep 71

BELLCOMM, INC.
955 L'ENFANT PLAZA NORTH, S.W., WASHINGTON, D.C. 20024

COVER SHEET FOR TECHNICAL MEMORANDUM

TITLE- Stability and Response of the CMG-Controlled Flexible Skylab

TM- 71-1022-5

DATE- September 17, 1971

FILING CASE NO(S)- 620

AUTHOR(S)- P. G. Smith

FILING SUBJECT(S) (ASSIGNED BY AUTHOR(S))- Attitude Control
Spacecraft Flexibility
Crew Motion Disturbances

ABSTRACT

By use of a mathematical model of the Skylab structure and CMG control system, it is shown that typical continuous crew motions, such as operation of a control console, give rise to 1-3 arc sec rms attitude excursions and 2-5 arc sec/sec rms attitude rates. These values are well within the tolerance of the hardmounted experiments on board, and thus crew motions of the type considered are permissible during observation periods. Furthermore, the attitude excursions obtained are substantially smaller than those obtained previously for isolated crew motions, such as wall push-offs, and it now appears that with appropriate crew motion constraints, useful ATM experiment data could be obtained even if the Experiment Pointing and Control Subsystem should fail.

The stability results (gain margins) obtained agree well with those obtained by the Martin Marietta Corporation. In view of the complementary nature of the two models - one concentrates on vehicle dynamics detail whereas the other concentrates on control system detail - and in view of the fact that the two investigations make use of independently generated vibration data, the agreement provides additional confidence in the control system design adequacy. The bending filters (feedback compensation) included in the control system are shown to be necessary to ensure system stability in view of uncertainties in structural flexibility and damping.

The mathematical model, written in state variable form, includes the vibrational modes of the structure (about 40 modes), the bending filters, the sensor and CMG dynamics, and spectrum shaping filters used in connection with the crew motion. Stability is determined from the eigenvalues of the system matrix, and response is obtained from the state covariance matrix.

The vibration modes used are selected from the available ones on the basis of how they influence system eigenvalues, in particular, on their potential for driving eigenvalues into the right half plane.

Bellcomm

955 L'Enfant Plaza North, S.W.
Washington, D. C. 20024

date: September 17, 1971

to: Distribution

from: P. G. Smith

subject: Stability and Response of the CMG-Controlled Flexible Skylab
Case 620

TM-71-1022-5

TECHNICAL MEMORANDUM

Introduction

The behavior of the flexible Skylab spacecraft when acted upon by external forces and torques and especially when under the influence of the CMG (control moment gyroscope) feedback control system has long been a topic of interest to those concerned with the vehicle's attitude motion. Although analysis and design of the CMG system has generally proceeded under the assumption of a rigid vehicle, so-called bending filters were added to the control loops as early as 1967 to suppress vibrations expected in the flexible vehicle. The bending filter design is reviewed periodically as new vibration data become available. In January of this year the entire topic of controlling a flexible Skylab was reviewed by the Skylab Program Director [1], and the topic received further attention in April at a Skylab Subsystem Review [2].

Control system performance is measured primarily in terms of control loop stability and response to worst case transient excitations, such as crew wall push-offs. Investigators with optical experiments on board, however, are more concerned with spacecraft response to typical continuous excitations, such as crew operation of a control console. This memorandum deals with both control loop stability and response to a continuous random excitation.

System Equations

We desire to represent the flexible spacecraft, the control system (including the bending filters), and the excitation in terms of a set of linear, first-order ordinary differential equations

$$\dot{x}(t) = Ax(t) + Bw(t) \qquad (1)$$

where x(t) is the N-element state vector, A is an N x N coefficient matrix, w(t) is a vector of independent white noise processes that drive the system, and B is the input coefficient matrix.* We proceed now to generate A by writing all of the dynamical equations in the proper form and by combining these equations so as to obtain the single matrix equation (1).

Figure 1 shows the major components of the model. Two sets of equations will be written, one for use when crew motion acts as the excitation and the other for use when sensor noise acts as the excitation; this does not restrict the usefulness of the equations, for the response to both excitations acting simultaneously can be obtained by superposition. The state

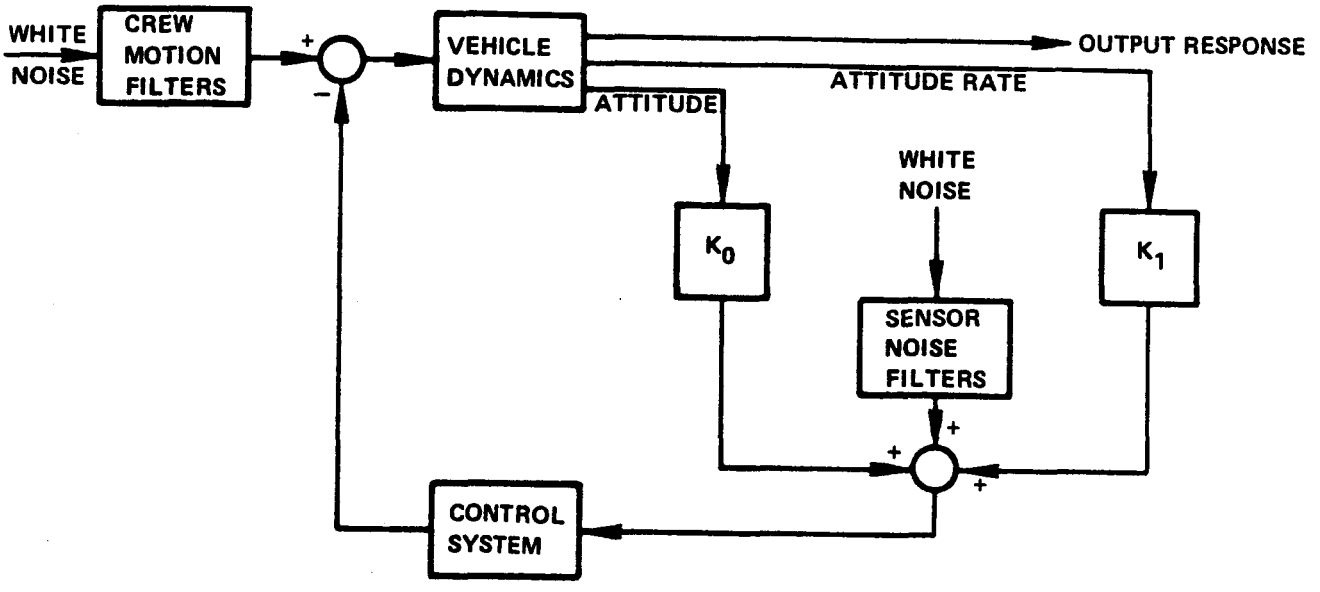

Figure 1. System block diagram

*A more complete representation would include difference equations as well to model the digital control system. To the extent that system frequencies are small compared to the 5 samples/sec sampling rate, however, the continuous model (1) is satisfactory.

vector x is partitioned into subvectors $x_1,\ldots,x_4$, which are associated with the vehicle dynamics, $\hat{x}$, which is associated with the control system,* and $\tilde{x}$, which is associated with either the crew motion or the sensor noise excitation filters ($\tilde{x}$ will be further partitioned later).

Vehicle Dynamics - Available modal analyses are used to represent the flexible vehicle dynamics. The normal modes of vibration, denoted by the transformation matrix Φ, are modified as shown in Appendix A to yield a modified transformation matrix Ψ. The first six columns of Ψ represent, respectively, rigid body x-translation, y-translation, z-translation, x-rotation, y-rotation, and z-rotation; the remaining columns represent the conventional elastic normal modes. The motivation for using Ψ rather than Φ is that rigid body translations, which would give rise to mathematical difficulties later on, are now available explicitly and can be eliminated from the equations of motion.

It should be kept in mind that Ψ represents a transformation between modal coordinates, that is, specific modes of vibration, and physical coordinates, that is, translations along or rotations about orthogonal axes at specific locations on the structure. Let M_1' denote the number of locations at which the crewman might be located, and let M_1 denote the number of that location at which he is currently located ($1 \leq M_1 \leq M_1'$); let M_2 denote the number of locations at which output response is desired, and let n denote the number of modes used. Then Ψ is a $(6M_1'+3M_2+9)$ x n matrix whose rows are organized as shown in Table I.

---

*The control system can include the bending filters and the dynamics of the sensors and the CMGs; various combinations of these elements are to be investigated.

Table I

Organization of rows of Ψ

rows start	rows end	number of rows	function	order within group
1	3	3	actuators (CMGs)	$\theta_x \theta_y \theta_z$
4	6	3	attitude sensors	$\theta_x \theta_y \theta_z$
7	9	3	rate sensors	$\theta_x \theta_y \theta_z$
10	$6M_1'+9$	$6M_1'$	crew locations	$xyz\theta_x\theta_y\theta_z$ for each loc.
$6M_1'+10$	$6M_1'+3M_2+9$	$3M_2$	output	$\theta_x \theta_y \theta_z$ for each loc.

It is convenient to deal with submatrices Ψ_i of Ψ, as shown in Table II.

Table II

Definition of submatrices Ψ_i

i	rows of Ψ start	rows of Ψ end	columns of Ψ start	columns of Ψ end
1	$6M_1+4$	$6M_1+9$	4	6
2	$6M_1+4$	$6M_1+9$	7	n
3	1	3	7	n
4	4	6	7	n
5	7	9	7	n
6	1	9	4	n
	$6M_1+7$	$6M_1+9$		
	$6M_1'+10$	$6M_1'+3M_2+9$		

If x_1 is a 3 x 1 vector denoting rigid body rotations of the vehicle and if x_3 is its derivative, then the rigid body rotation equations of motion are*

$$\dot{x}_1 = x_3 \tag{2}$$

$$I\dot{x}_3 = \Psi_1^T f_e + t_c \tag{3}$$

where I is the 3 x 3 centroidal inertia matrix, which may be obtained from the rigid body modes (see Appendix B), f_e is a 6 x 1 vector denoting the crew excitation forces and torques, if any, and t_c is a 3 x 1 vector denoting the control torque.

If x_2 is an (n-6) x 1 vector denoting the elastic modal coordinates and if x_4 is its derivative, then equations for the elastic motions are

$$\dot{x}_2 = x_4 \tag{4}$$

$$\dot{x}_4 + Dx_4 + \Lambda x_2 = \Psi_2^T f_e + \Psi_3^T t_c \tag{5}$$

where $D = \text{diag}\,(2\zeta\omega_7, \ldots, 2\zeta\omega_n)$ and $\Lambda = \text{diag}\,(\omega_7^2, \ldots, \omega_n^2)$, ζ being the structural damping ratio and ω_i, i=7, ..., n, being the vibration frequencies.

Note that because rigid body translations (modes 1-3) are excluded, only n-3 of the n columns of Ψ are actually used.

---

*Superscript T denotes matrix transposition.

Control System - We assume that the feedback is uncoupled (between control axes) and linear, in which case the control system can be represented in Laplace transform notation as

$$H_1(s) = -\left(\sum_{i=1}^{\ell-1} P_i s^i\right)\left(E_3 s^{\ell} + \sum_{i=0}^{\ell-1} Q_i s^i\right)^{-1} \tag{6}$$

where P_i and Q_i are diagonal 3 x 3 coefficient matrices (E_n denotes the n x n identity matrix). $H_1(s)$ (also 3 x 3 diagonal) is the transfer function between the control variable u(s),*

$$u = K_0(x_1 + \Psi_4 x_2) + K_1(x_3 + \Psi_5 x_4) + n_s \tag{7}$$

and the control torque $t_c(s)$. The state variable representation of (6) is

$$\dot{\hat{x}} = \hat{A}\hat{x} + \hat{B}u \tag{8}$$

$$t_c = \hat{C}\hat{x} \tag{9}$$

where

$$\hat{A} = \begin{bmatrix} 0 & E_3 & & & \\ 0 & 0 & E_3 & & \\ \vdots & & \ddots & \ddots & \\ & & & & E_3 \\ -Q_0 & -Q_1 & -Q_2 & \cdots & -Q_{\ell-1} \end{bmatrix}, \quad \hat{B} = \begin{bmatrix} 0 \\ 0 \\ \vdots \\ -E_3 \end{bmatrix}$$

$$\hat{C} = \begin{bmatrix} P_0 & P_1 & P_2 & \cdots & P_{\ell-1} \end{bmatrix} \tag{10}$$

---

*K_0 and K_1 are diagonal 3 x 3 position and rate gain matrices, respectively, as shown in Figure 1, and n_s denotes the sensor noise, which will be described later.

Excitation Filters - As mentioned earlier, these are handled in two different ways depending on whether the excitation is due to crew motion or sensor noise. For crew motion we postulate six independent third-order filters (three filters for the forces and three for the torques exerted by a single crewman), and thus $\tilde{x}$ is partitioned into three 6 x 1 subvectors x_a, x_b and x_c. In transfer function notation the filters take the form

$$H_2(s) = \tilde{A}s^2(E_6s^3+\tilde{B}s^2+\tilde{C}s+\tilde{D})^{-1} \tag{11}$$

where $\tilde{A}$, $\tilde{B}$, $\tilde{C}$, $\tilde{D}$ are all diagonal 6 x 6 coefficient matrices. In state variable notation they take the form

$$\dot{x}_a = x_b \tag{12}$$

$$\dot{x}_b = x_c \tag{13}$$

$$\dot{x}_c = -\tilde{D}x_a-\tilde{C}x_b-\tilde{B}x_c+w(t) \tag{14}$$

$$f_e = \tilde{A}x_c \tag{15}$$

where w(t), 6 x 1, is the driving function introduced in (1). The sensor noise, $n_s=0$.

For sensor noise excitation three second-order filters are used, one for each control axis. In this case $f_e=0$; $\tilde{x}$ is partitioned into two 3 x 1 subvectors x_a and x_b; $\tilde{A}$, $\tilde{B}$, $\tilde{C}$, $\tilde{D}$ are 3 x 3 diagonal matrices; and w(t) is 3 x 1. The transfer function is now

$$H_3(s) = (\tilde{A}s+\tilde{B})(E_3s^2+\tilde{C}s+\tilde{D})^{-1} \tag{16}$$

and the state variable representation is

$$\dot{x}_a = x_b \tag{17}$$

$$\dot{x}_b = -\tilde{D}x_a-\tilde{C}x_b+w(t) \tag{18}$$

$$n_s = \tilde{B}x_a+\tilde{A}x_b \tag{19}$$

Single Matrix Equation - The only remaining task is to combine all of the preceeding equations into a single equation of form (1). This is done for each of the two types of excitation.

When crew motion excitation is used

$$N = 2n + 3\ell + 12 \tag{20}$$

and the N x N matrix A is partitioned into an 8 x 8 array of submatrices corresponding to the eight subvectors $x_1, x_2, x_3, x_4, \hat{x}, x_a, x_b, x_c$ of x.

$$A = \begin{bmatrix} & & E_3 & & & & & \\ & & & E_{n-6} & & & & \\ & & & & I^{-1}\hat{C} & & I^{-1}\psi_1^T\tilde{A} & \\ & -\Lambda & & -D & \psi_3^T\hat{C} & & \psi_2^T\tilde{A} & \\ \hat{B}K_0 & \hat{B}K_0\psi_4 & \hat{B}K_1 & \hat{B}K_1\psi_5 & \hat{A} & & & \\ & & & & & E_6 & & \\ & & & & & & E_6 & \\ & & & & -\hat{D} & -\hat{C} & -\hat{B} & \end{bmatrix} \tag{21}$$

$$B^T = [0\ 0\ \ldots\ 0\ E_6] \tag{22}$$

When sensor noise excitation is used

$$N = 2n + 3\ell \tag{23}$$

In this case there is no x_c so A is partitioned into a 7 x 7 array of submatrices.

$$A = \left[\begin{array}{ccc|c|c|cc} & & & E_3 & & & \\ & & & & E_{n-6} & & \\ & & & & & I^{-1}\hat{C} & \\ & -\Lambda & & & -D & \Psi_3^T\hat{C} & \\ \hat{B}K_0 & \hat{B}K_0\Psi_4 & \hat{B}K_1 & \hat{B}K_1\Psi_5 & & \hat{A} & \hat{B}\tilde{B} \quad \hat{B}\tilde{A} \\ & & & & & & E_3 \\ & & & & & & -\tilde{D} \quad -\tilde{C} \end{array}\right] \tag{24}$$

$$B = \left[0 \; 0 \; . \; . \; . \; 0 \; E_3\right] \tag{25}$$

Selection of Vibration Modes

Available modal analyses provide more vibration modes than can be accommodated by computer core storage, so it is necessary to select the "most important" modes from the available ones and to use only these to construct the A matrix. Modes are selected here on the basis of how they affect eigenvalues of A. Experience indicates that it is usually* possible to associate with each elastic mode used a specific complex pair of eigenvalues of A simply by comparing the resonant frequency of the mode (in rad/sec) with the imaginary part of the eigenvalue. Once this is done the effect of each mode on system stability can be evaluated by examining the real part of the associated eigenvalue.

*The association can be obscured for some modes if their resonant frequencies are close.

Gevarter [3] shows by means of a simple model that the real part of a modal eigenvalue is the sum of two parts, that part due to structural damping and that part arising from control feedback. The former part is always negative, but the latter can be of either sign depending on both the modeshape and the feedback characteristics. The present model is more complicated than the one analyzed by Gevarter, but the eigenvalues nevertheless seem to behave as predicted by the simple model. Moreover, this behavior suggests the modal importance criterion about to be described.

Suppose that the eigenvalue pair λ_i,

$$\lambda_i = -a_i \pm jb_i \tag{26}$$

$i = 7, \ldots, n$, $j = \sqrt{-1}$, $b_i > 0$, can be associated with the ith mode of vibration. In accordance with the aforementioned behavior, suppose that a_i is composed of two parts, $a_i = a_{si} + a_{ci}$, where a_{si} is the contribution of structural damping, $a_{si} = \zeta b_i$, and a_{ci} is the control contribution. Our criterion for modal importance is that unimportant modes are those for which damping is influenced relatively little by the control system, quantitatively $|a_{ci}| << a_{si}$, or expressed in terms of the available values, a_i, b_i and ζ,

$$\left| \frac{a_i}{\zeta b_i} - 1 \right| << 1 \tag{27}$$

Another possible criterion and its deficiency should be mentioned. The criterion is that the control should enhance modal damping as much as possible. Under this criterion a mode with a large positive a_{ci} should be less troublesome than one with a small a_{ci}. The deficiency, however, is that a_{ci} depends on loop gain, specifically, gain at the mode's resonant frequency. A different control can change the sign of the gain at the resonant frequency, thus changing a mode with a troublefree large positive a_{ci}

to one with a troublesome large negative a_{ci}. That is to say, a mode whose damping is capable of being enhanced by the control is also susceptible to having its damping annihilated by the control.

Control system performance is investigated here using each of five different modal analyses; these are described in Table III. Each modal analysis has been processed to select the 33* most important modes out of the 120 or so that are available, and the results are presented in Table IV. (Inasmuch as only 33 modes can be accommodated at once, it is necessary to process each set of modes in several batches of 33 or less modes each.)

Table IV was obtained using a control system of the form $300K_{DC}/(s + 300)$ on each of the three control axes, where K_{DC} is the DC gain of the bending filters in Reference 5.** Because the characteristic frequencies of the system are small compared to 300, the effect of the control system is essentially to multiply the feedback by the constant K_{DC}. The reason for using low pass filters with a high break frequency as a control system is that they fit the established analytical framework while essentially providing direct feedback. Direct feedback is desired to eliminate the bias of any particular control system in determining modal importance.

---

*Computer capacity is 33 elastic modes.

**The 300 value was raised to 3000 for the MMC226 modal analysis on account of a few unusually high resonant frequencies encountered therein.

Table III

Modal analyses used

Name	Source	Remarks
HESNOM	H. E. Stephens	Standard or "nominal" stiffness and mass values
HESK8	H. E. Stephens	Stiffness of Deployment Assy. (DA) reduced 20%
HESM12	H. E. Stephens	Mass of ATM increased 20%
HESMK	H. E. Stephens	20% reduction in DA stiffness and 20% increase in ATM mass
MMC226	Martin Marietta 2/26/71 [4]	Used to design bending filters

In summary, Table IV lists elastic modes in decreasing order of their potential for causing instability. In the sequel, vehicle flexibility will be represented by use of all the 33 modes listed.

Stability Results

Stability is determined from the eigenvalues of the A matrix: for stability the real parts of all eigenvalues must be negative.*

*Owing to the fact that the excitation filters do not affect control stability,only the eigenvalues of a matrix comprising the first $2n + 3\ell - 6$ rows and columns of A need actually be computed.

TABLE IV

Frequency, ω_i (Hertz), and importance parameter, $h_i = \left| \frac{a_i}{\zeta b_i} - 1 \right|$,

for five modal analyses

ORDER	HESNOM			HESK8			HESM12			HESMK			MMC226		
	Mode	ω_i	h_i	Mode	ω_i	h_i	Mode	ω_i	h_i	Mode	ω_i	h_i	Mode	ω_i	h_i
1	31	.9	82.	29	.8	107.	30	.9	84.	29	.8	108.	27	.9	63.
2	37	1.2	1.3	114	9.2	2.1	78	5.1	1.8	62	2.9	3.4	106	9.6	51.
3	28	.7	1.2	47	2.0	1.4	54	2.3	1.5	65	3.5	1.8	107	11.	26.
4	54	2.4	1.2	28	.7	1.3	24	.7	1.2	24	.7	1.4	98	6.5	13.
5	96	7.2	1.0	71	4.2	1.2	38	1.4	1.2	93	6.6	1.3	113	36.	13.
6	70	4.2	.86	52	2.3	1.2	93	6.8	.91	52	2.2	1.2	48	1.6	13.
7	63	3.4	.78	63	3.0	1.0	63	3.1	.82	38	1.4	1.1	39	1.2	1.6
8	85	5.6	.74	68	3.9	.99	64	3.4	.75	75	4.5	.98	99	6.9	1.5
9	24	.7	.72	65	3.5	.91	65	3.7	.67	47	2.1	.92	97	6.0	1.4
10	19	.6	.66	97	7.1	.88	19	.6	.64	66	3.8	.68	71	4.3	1.1
11	64	3.7	.58	24	.7	.75	28	.7	.58	19	.6	.61	38	1.2	.88
12	47	2.1	.51	37	1.3	.75	66	3.8	.57	74	4.4	.58	55	2.4	.59
13	69	4.1	.30	19	.6	.62	71	4.2	.55	28	.7	.48	96	5.9	.53
14	113	9.1	.25	92	6.1	.30	44	1.8	.34	78	4.9	.47	95	5.8	.52
15	86	5.7	.24	20	.6	.27	105	8.4	.29	64	3.3	.40	110	18.	.48
16	44	1.7	.22	55	2.4	.24	20	.6	.29	71	4.1	.40	42	1.3	.38
17	20	.6	.22	78	5.3	.23	43	1.6	.26	20	.6	.35	40	1.3	.34
18	60	2.7	.20	64	3.3	.21	77	4.8	.18	48	2.2	.34	88	5.0	.32
19	84	5.6	.20	118	9.4	.19	86	5.6	.17	105	8.4	.33	114	48.	.31
20	76	5.0	.18	86	5.6	.16	82	5.4	.15	44	1.7	.23	44	1.4	.31
21	62	3.2	.16	44	1.7	.11	74	4.4	.14	43	1.6	.17	14	.5	.31
22	73	4.4	.16	38	1.3	.10	92	6.1	.13	86	5.6	.15	112	30.	.26
23	75	4.7	.14	43	1.6	.10	70	3.9	.12	92	6.1	.14	10	.2	.25
24	101	7.5	.13	82	5.4	.09	37	1.3	.11	57	2.7	.12	56	2.5	.22
25	38	1.3	.11	119	9.4	.09	39	1.5	.10	109	8.5	.10	62	3.1	.21
26	77	5.4	.08	77	4.7	.09	109	8.5	.08	73	4.3	.09	43	1.4	.21
27	39	1.5	.08	69	3.9	.09	40	1.6	.06	37	1.3	.09	70	3.9	.13
28	43	1.6	.07	40	1.6	.07	36	1.1	.06	60	2.7	.08	108	13.	.13
29	90	6.0	.06	75	4.7	.07	48	2.2	.05	7	.2	.08	49	2.3	.12
30	36	1.1	.06	74	4.4	.06	45	1.8	.05	40	1.6	.08	28	1.0	.12
31	40	1.6	.06	61	2.8	.06	51	2.2	.05	39	1.5	.08	31	1.0	.11
32	51	2.2	.05	39	1.5	.05	75	4.7	.05	36	1.1	.05	64	3.7	.10
33	81	5.5	.05	102	7.5	.05	87	5.7	.04	70	3.9	.04	41	1.3	.08

Table V shows stability results for four conditions without bending filters. The conditions are ζ=.01 (standard structural damping) and ζ=.001 (light damping), each with direct feedback (see p. 11) and with a control system comprising just sensor prefilters of the form 31.4/(s+31.4) on each axis and CMG dynamics filters of the form 30/(s+30) on each axis [6]. With one exception (mode

Table V

Stability results without bending filters

(Where stability does not prevail, the mode numbers responsible are indicated.)

control system	ζ	HESNOM	HESK8	HESM12	HESMK	MMC226
direct feedback	10^{-2}	stable	stable	stable	stable	113
direct feedback	10^{-3}	stable	stable	stable	stable	113
prefilters & CMG	10^{-2}	stable	stable	stable	stable	106,107
prefilters & CMG	10^{-3}	96	97,114	93	93	49,96-99, 106,107

49 of the Martin analysis), instability is attributable to higher modes (above 5 Hz), which, because of modeling uncertainties, are of dubious accuracy. Due to this uncertainty it is not possible to state whether or not the flight vehicle would be stable without bending filters, and thus bending filters are required to ensure stability of the flight hardware.

When the control system comprises bending filters [5]* in addition to the prefilters and CMG dynamics already mentioned, stability is obtained for all five modal analyses. Table VI gives the gain margins, that is, the largest factors by which

*The bending filter transfer function is derived in Appendix C.

all gains in Reference 5 (elements of K_0 and K_1) can be multiplied without loosing stability. The bending filters are designed to yield a gain margin of at least 10 db, and it is apparent from the table that that objective is attained for all five modal analyses.

Table VI

Gain margins

Modal analysis	Gain margins	
	flexible body	rigid body
HESNOM	4.3 (12.7 db)	3.5 (10.9 db)
HESK8	4.8 (13.6 db)	3.5 (10.9 db)
HESM12	4.7 (13.4 db)	3.6 (11.1 db)
HESMK	4.9 (13.8 db)	3.6 (11.1 db)
MMC226	4.8 (13.6 db)	3.7 (11.4 db)

Response Results

The desired rms response can be obtained from the state covariance matrix,*

$$X(t) = E\{x(t)x^T(t)\} \tag{28}$$

in particular, from its asymtotic value, $X = \lim_{t\to\infty} X(t)$, which is the solution of the matrix equation [7]

$$AX + XA^T + BB^T = 0 \tag{29}$$

---

*$E\{\cdot\}$ denotes the expectation operator. It is assumed that $E\{x(0)\} = E\{w(t)\} = 0$, in which case it follows from (1) that $E\{x(t)\} = 0$ for all $t>0$.

for X. Matrices A and B are defined by (21) and (22) (crew motion excitation) or by (24) and (25) (sensor noise excitation); and means are available for solving (29) numerically [8].

Solutions of (29) are not unique if any eigenvalues of A have zero real parts. Such eigenvalues arise from rigid body translation, and this is why rigid body translation has been suppressed by using the modal transformation matrix Ψ rather than Φ.

State vector x involves the vehicle modal coordinates rather than the physical coordinates needed for output. Let y,

$$y = Cx \tag{30}$$

be the desired output variables (coordinates), that is, the attitude and attitude rate at certain specified locations on the vehicle. The transformation is (see Table II)

$$C = \begin{bmatrix} \Psi_6 & 0 & 0 \\ 0 & \Psi_6 & 0 \end{bmatrix} \tag{31}$$

and the covariance of y, $Y = E\{y\ y^T\}$, is

$$Y = C\ X\ C^T \tag{32}$$

Rms response is obtained by taking square roots of the diagonal elements of Y.

Reference 9 gives measured power spectral density data for a variety of crew activities, and for most of these activities the power spectral densities can be adequately represented by the third-order filters (11).* The most vigorous activity that will fit into form (11) is one called shower preparation.

---

*Although second-order filters, such as those proposed in Reference 9, may fit the measured data well, they are unsatisfactory in the present application inasmuch as they give rise to unbounded mean square response in either force or displacement.

Table VII shows spacecraft rms attitude response to the shower preparation activity being performed in the living quarters of the OWS. It is apparent from this table that rigid body motion predominates. Observe that the response is essentially the same at the CMG location in the ATM, at the location of experiment S192 in the MDA, and at the location of experiment S019 in the OWS. Also observe that response for the HESNOM modes is about the same for the rigid body modes alone as it is for the rigid body plus elastic modes; moreover, the results are essentially independent of which modal analysis is used, at least among the HES analyses.

Table VII

Response to shower preparation excitation in the OWS

(arc second units)

Modal analysis	ATM (CMG)	MDA (S192)	OWS (S019)
HESNOM	3.3	3.2	3.2
{HESNOM rigid body}	3.0	3.0	3.0
HESK8	3.4	3.2	3.2
HESM12	3.4	3.2	3.2
HESMK	3.5	3.2	3.2
MMC226	5.1	5.0	5.0

In view of these findings, we work henceforth with just one modal analysis - HESNOM - and with just one output location - that of S192 in the MDA. Table VIII provides detailed response data for several types of excitation. Console operation [9] is typical of a mild crew motion. Crew motion in the MDA gives rise to smaller response by

virtue of the smaller lever arms involved.* The last two lines of Table VIII are included to show that crew motion dominates the random disturbance stemming from sensor noise.**Statistics for rate gyro noise are obtained

Table VIII

MDA response using HESNOM modes
(arc second and arc second/sec units)

excitation	x-axis		y-axis		z-axis		combined	
	angle	rate	angle	rate	angle	rate	angle	rate
shower prep. in OWS	0.99	2.2	2.3	4.1	2.0	2.1	3.2	5.1
console op. in OWS	0.83	1.6	0.82	1.3	1.5	1.2	1.9	2.4
console op. in MDA	1.1	3.1	0.41	0.77	0.76	0.89	1.4	3.3
rate gyro noise	.015	.003	.003	.001	.014	.002	.021	.004
sun sensor noise	.009	.002	.002	.001	.003	.001	.009	.002

by least-squares fitting measured data† to form (16); for the sun sensor a measured rms noise value†† is used, and the noise is assumed to exist between 10 and 20 Hz. The columns in Table VIII give rms attitude and attitude rate for the x y and z axes individually and combined (root sum square).

---

*If the spacecraft were very flexible, response would tend to be largest in the vicinity of the excitation, and thus MDA excitation would yield larger MDA response.

**Gyro drift is not included because it may be treated as a deterministic disturbance.

†Specifically, measured power spectral densities, supplied by E. H. Fikes, MSFC, for gyros, serial nos. 112, 113, 114, 117, 121, are used.

††Supplied by W. L. Kimmons, MSFC.

Excessive attitude excursions and attitude rates can impair the performance of certain experiments on board. Table IX lists the most critical Skylab experiments in this regard.* From comparison of Tables VIII and IX it is clear that the type of crew motions considered here will not degrade experiment performance.**

Table IX

Experiment pointing requirements

Experiment	Requirement	Basis for requirement
S019 UV Stellar Astronomy	20 arc sec	Experiment Requirements Document for UV Stellar Astronomy, MSC, Sept. 1970
S190 Multispectral Photographic Facility	10^3 arc sec/sec	Resolution of 7×10^{-5} rad and shutter speed of 10^{-2} sec
S191 Infrared Spectrometer	300 arc sec	Maintain 1/4 mi IFOV inside 1 mi target area
S192 Multispectral Scanner	200 arc sec/sec	Move 5% of IFOV during one scan

Summary and Conclusions

The mathematical model developed here provides considerable detail in regard to both control system and vehicle dynamics. The control system provides for bending filters (feedback compensation) and sensor and actuator dynamics of arbitrary order. The vehicle dynamics are three-dimensional and can be represented by up to about forty vibration modes. The spatial detail provided is illustrated by the fact that the x, y and z axis

*ATM experiments are isolated from spacecraft motions, and so they are not considered here.

**Certain vigorous deterministic crew motions give rise to larger attitude perturbations that are of concern to principal investigators [10].

rate sensors are all mounted at different locations. The only significant difference between the mathematical model and the flight hardware is the use of a continuous rather than discrete control system, but this is justifiable on the grounds that the Skylab sampling rate is high relative to most characteristic frequencies and by the fact that the bending filters provide great attenuation at frequencies approaching the sampling rate.

Insofar as the writer is aware, a new means is presented for selecting the vibration modes to be used. Selection is based not on the properties of the modes themselves (deflections, slopes and frequencies), as is commonly done, but rather on how the modes influence system eigenvalues. Specifically, modes are rated on their potential for causing instability. The new method has the advantage that it is decisive: the effects of feedback and interaxis coupling are included automatically,and the relative importance of various axes is taken care of, as is dependence on vibration frequency.

System stability is checked with and without the bending filters. Without the filters the system can be either stable or unstable, depending on which modal analysis is used and how much structural damping is provided. Bending filters are required, therefore, to ensure stability in view of the uncertainties in the modal analyses and structural damping.

With bending filters, gain margins of at least 3.5 (11 db) are obtained for all five of the modal analyses used; these results are in line with those obtained by Martin Marietta Corporation. In view of the differences between the Martin model and the present one (Martin concentrates on control system detail, whereas vehicle dynamics detail is emphasized herein) and the differences in the modal data used (Martin uses their own data, whereas that of Stephens is used primarily here) the good agreement in the gain margins reinforces confidence in the control system design.

Skylab attitude response is obtained for various random excitations. It is found that the response is primarily due to rigid body modes, and thus vehicle flexibility has a greater impact on stability of the attitude motion than on the motion itself.

Typical continuous crew motions, such as console operation and preparation of a shower facility, give rise to attitude excursions of 1-3 arc seconds rms and attitude rates of 2-5 arc seconds/second rms. A survey of the experiments carried on Skylab reveals that the strictest attitude requirement is 20 arc seconds (S019) and the strictest rate requirement is 200 arc seconds/second (S192). Therefore, crew motions of the type considered are permissible during observation periods.

The attitude excursions reported here for continuous crew motions are about fifty times smaller than those reported previously for isolated crew motions, such as wall push-offs [2], [5]. It now appears that with appropriate crew motion constraints some useful data could be obtained from the ATM even if the gimbals were locked due to Experiment Pointing and Control Subsystem failure.

Attitude excursions arising from sensor noise are found to be negligible.

Acknowledgement

Credit for the numerical aspects of this project is due to Ron Grutzner, who did the programming, and to Hank Stephens, who prepared most of the modal data.

Preston G. Smith

P. G. Smith

1022-PGS-$^{tla}_{mef}$

Attachments

Appendix A

Eliminating Rigid Body Translation from a Modal Analysis

Modal data for a free structure, such as a spacecraft, comprises two parts, rigid body modes and elastic modes. Due to constraints placed on the rigid body modes by orthogonality, these modes are not pure motions, that is, each mode represents a combination of translation and rotation involving all three axes. The present objective is to obtain from given rigid body modes six modes that do represent pure motions (but are not orthogonal); then rigid body translations can be identified and suppressed, as required in the body of the memorandum.

Assume that the structure is modeled using m degrees of freedom and that each of the associated variables, $u_i, i=1,\cdots,m$, constitutes an x,y or z displacement or an x,y or z rotation at a point in the structure whose location is (p_i,q_i,r_i) relative to composite mass center. Let F be an m×1 vector, $F^T=[f_1\cdots f_m]$, whose elements f_i are forces or torques corresponding to u_i; for example, if u_i is a y-rotation, f_i is a torque about the y-axis applied at (p_i,q_i,r_i). The linear equations of motion are

$$M\ddot{u} + Ku = F \tag{A-1}$$

where M is the m×m symmetric mass matrix and K is the m×m symmetric stiffness matrix.

A transformation of variables exists that will simultaneously diagonalize M and K, and with such transformation (A-1) takes the form

$$\ddot{\xi} + \Lambda\xi = \Phi^T F \tag{A-2}$$

$$u = \Phi\xi \tag{A-3}$$

where use is made of

$$\Phi^T M \Phi = E_m \text{ (identity matrix)} \tag{A-4}$$

$$\Phi^T K \Phi = \Lambda \text{ (diagonal)} \tag{A-5}$$

Although in principle Φ is m×m, in practice one usually has access to only $n \leq m$ columns of Φ, so it is assumed henceforth that Φ has been truncated to m×n and ξ to n×1, $6 \leq n \leq m$.

Because the structure is free, Λ has six zero diagonal elements. Let Φ (and thus ξ) be organized so that the zero diagonal elements of Λ appear first, followed by the n-6 nonzero ones:

$$\Lambda = \begin{bmatrix} 0_6 & \\ & \Lambda'' \end{bmatrix} \tag{A-6}$$

Thus the first six columns of Φ constitute independent rigid body motions, and the specification of $\xi_1, \cdots, \xi_6$ is sufficient to define any small rigid body motion.

Let

$$\xi = \begin{bmatrix} \xi' \\ \xi'' \end{bmatrix} \quad , \quad \xi'^T = [\, \xi_1 \cdots \xi_6 \,] \quad , \quad \xi''^T = [\, \xi_7 \cdots \xi_n \,] \tag{A-7}$$

and introduce another set of rigid body coordinates $\eta, \eta^T = [\eta_1 \cdots \eta_6]$, such that η_1, η_2, η_3 are xyz translations of the vehicle mass center, respectively, and η_4, η_5, η_6 are xyz rigid body rotations, respectively. Because either ξ' or η is sufficient to define rigid body motions, there exists a nonsingular transformation between them,

$$\xi' = Q\eta \quad \text{or} \quad \eta = P\xi', \quad P = Q^{-1} \tag{A-8}$$

If $\hat{u}$ denotes the rigid body portion of u, then by (A-3) and (A-8)

$$\hat{u} = \Phi' \xi' = \Phi' Q \eta \tag{A-9}$$

where Φ' denotes the first six columns of Φ.

Another relation between $\hat{u}$ and η, namely

$$\hat{u} = T\eta \tag{A-10}$$

can be obtained on purely kinematical grounds.

Recall that each element u_i of u is an x,y or z translation or rotation at the location (p_i,q_i,r_i), Consequently,

$$\hat{u}_i = \begin{cases} [1 \quad 0 \quad 0 \quad 0 \quad r_i \quad -q_i]\eta \text{ if } u_i \text{ is x translation} \\ [0 \quad 1 \quad 0 \quad -r_i \quad 0 \quad p_i]\eta \text{ if } u_i \text{ is y translation} \\ [0 \quad 0 \quad 1 \quad q_i \quad -p_i \quad 0]\eta \text{ if } u_i \text{ is z translation} \\ [0 \quad 0 \quad 0 \quad 1 \quad 0 \quad 0]\eta \text{ if } u_i \text{ is x rotation} \\ [0 \quad 0 \quad 0 \quad 0 \quad 1 \quad 0]\eta \text{ if } u_i \text{ is y rotation} \\ [0 \quad 0 \quad 0 \quad 0 \quad 0 \quad 1]\eta \text{ if } u_i \text{ is z rotation} \end{cases} \tag{A-11}$$

and T can be generated by rows by picking the proper line of (A-11) for each u_i, i=1,···,m, according to the way in which u is organized. Because (A-9) and (A-10) hold for arbitrary η, it follows that

$$T = \Phi' Q \tag{A-12}$$

Suppose that one location in the structure is assigned a full six degrees of freedom. Let Φ^* comprise the corresponding six rows of Φ' in the order xyz translation, xyz rotation, and generate a T^* as described above using (p^*,q^*,r^*). Then in view of (A-11) and (A-12)

$$T^* = \begin{bmatrix} E_3 & -R^* \\ 0 & E_3 \end{bmatrix} = \Phi^* Q \tag{A-13}$$

where

$$R^* = \begin{bmatrix} 0 & -r^* & q^* \\ r^* & 0 & -p^* \\ -q^* & p^* & 0 \end{bmatrix} \tag{A-14}$$

Rearrangement of (A-13) and use of (A-8) yields

$$P = \begin{bmatrix} E_3 & R^* \\ 0 & E_3 \end{bmatrix} \Phi^* \qquad \text{(A-15)}$$

Equations (A-12) - (A-15) are useful in that with them T can be computed with less labor and with less knowledge of the structure than is indicated in (A-11). If one knows only that six specific elements of u are associated with a single location, he can compute the location, (p^*,q^*,r^*), (see Appendix B) and then use (A-14) to obtain R^*,(A-15) to obtain P, (A-8) to obtain Q, and finally (A-12) to obtain T. Given T, the modal transformation matrix Ψ used in the body of the memorandum is

$$\Psi = [T \qquad \Phi''] \qquad \text{(A-16)}$$

where Φ'' comprises columns 7 through n of Φ.

It remains to be shown that Ψ uncouples the equations of motion as desired so that the equations for rigid body translation can be deleted. Toward this end, apply Ψ to (A-1):

$$\Psi^T M \Psi \begin{bmatrix} \ddot{\eta} \\ \ddot{\xi}'' \end{bmatrix} + \Psi^T K \Psi \begin{bmatrix} \eta \\ \xi'' \end{bmatrix} = \Psi^T F \qquad \text{(A-17)}$$

By use of (A-16), (A-12) and (A-4) the first coefficient matrix becomes

$$\Psi^T M \Psi = \begin{bmatrix} T^T M T & T^T M \Phi'' \\ \Phi''^T M T & \Phi''^T M \Phi'' \end{bmatrix} = \begin{bmatrix} Q^T Q & 0 \\ 0 & E_{n-6} \end{bmatrix} \qquad \text{(A-18)}$$

and by use of (A-16), (A-12), (A-5) and (A-6) the second coefficient matrix becomes

$$\Psi^T K \Psi = \begin{bmatrix} T^T K T & T^T K \Phi'' \\ \Phi''^T K T & \Phi''^T K \Phi'' \end{bmatrix} = \begin{bmatrix} 0 & 0 \\ 0 & \Lambda'' \end{bmatrix} \tag{A-19}$$

Thus (A-17) uncouples into rigid body equations

$$Q^T Q \ddot{\eta} = T^T F \tag{A-20}$$

and elastic equations

$$\ddot{\xi}'' + \Lambda'' \xi'' = \Phi''^T F \tag{A-21}$$

The right hand side of (A-20) has a physical interpretation and to see this clearly F is cast into a new form by the introduction of the 3×1 vectors a_i and b_i, $i=1,\cdots,m$. Recall that the elements f_i of F are x,y or z forces or torques arranged according to the way in which u is organized. If f_i is a force, $b_i=0$ and f_i is set equal to the first, second or third element of a_i according to whether f_i is in the x, y or z direction, respectively. For example, if f_i is an x-direction force, $a_i^T = [f_i \ 0 \ 0]$ and $b_i = 0$. If f_i is a torque, then $a_i=0$ and f_i is similarly associated with b_i. Thus a_i and b_i represent forces and torques, respectively, associated with the i^{th} degree of freedom. By inspection of (A-11) it can be verified that

$$T^T F = \sum_{i=1}^{m} \begin{bmatrix} a_i \\ R_i a_i + b_i \end{bmatrix} \tag{A-22}$$

where

$$R_i = \begin{bmatrix} 0 & -r_i & q_i \\ r_i & 0 & -p_i \\ -q_i & p_i & 0 \end{bmatrix} \tag{A-23}$$

Now $\sum_{i=1}^{m} a_i$ is just the sum of the forces applied to the structure, and $\sum_{i=1}^{m} R_i a_i + b_i$ is the sum of the applied torques about the structure's mass center. Therefore, $T^T F$ is interpreted as the total applied force and torque relative to the structure's mass center.

If μ denotes the mass and I denotes the the centroidal inertia matrix of the complete structure, equations for the rigid body motion are

$$\begin{bmatrix} \mu E_3 & 0 \\ 0 & I \end{bmatrix} \ddot{\eta} = T^T F \tag{A-24}$$

in view of (A-22). Inasmuch as (A-20) and (A-24) must hold for any forces F and thus any accelerations $\ddot{\eta}$,

$$Q^T Q = \begin{bmatrix} \mu E_3 & 0 \\ 0 & I \end{bmatrix} \tag{A-25}$$

In view of (A-20), (A-21) and (A-25) it is clear that matrix Ψ transforms the equations of motion into a form in which equations for rigid body translation are uncoupled from the remaining equations.

Appendix B

Obtaining Rigid Body Inertia Data From a Modal Analysis

These data - composite mass, mass center location, and moments and products of inertia - are needed in the body of the memorandum and in Appendix A. It is best to obtain the data directly from the modal analysis, as this ensures that the data will be consistent with the modal analysis used.

The nomenclature used here corresponds with that of Appendix A, and the basic equations come from (A-2) and (A-3):

$$\ddot{\xi} + \Lambda\xi = \Phi^T F \tag{B-1}$$

$$u = \Phi\xi \tag{B-2}$$

Consider only rigid body motions of (B-1) and (B-2):

$$\ddot{\xi}' = \Phi'^T F \tag{B-3}$$

$$\hat{u} = \Phi' \xi' \tag{B-4}$$

Now suppose, as in Appendix A, that a single location is assigned a full six degrees of freedom. Let u*, a 6×1 vector, denote the translations and rotations associated with that location, and let F*, a 6×1 vector, denote the forces and torques applied at that location; assume that no other forces or torques are applied to the structure. Equations (B-3) and (B-4) become

$$\ddot{\xi}' = \Phi^{*T} F^* \tag{B-5}$$

$$u^* = \Phi^* \xi' \tag{B-6}$$

Differentiate (B-6) twice and substitute it into (B-5):

$$\ddot{u}^* = \Phi^* \Phi^{*T} F \tag{B-7}$$

Equation (B-7) gives the translation and rotation at one point on a rigid body when forces and torques are applied at that point. An equation relating u* and F* can also be derived from fundamental principles by using the mass, μ, the location of the point relative to the mass center, (p*,q*,r*), and the centroidal inertia Matrix, I, of the body. The result is

$$\begin{bmatrix} \mu E_3 & \mu R^* \\ -\mu R^* & I-\mu R^{*2} \end{bmatrix} \ddot{u}^* = F^* \qquad \text{(B-8)}$$

Now $\ddot{\mu}^*$ can be eliminated between (B-7) and (B-8), and because F* can take on arbitrary values it follows that

$$\begin{bmatrix} \mu E_3 & \mu R^* \\ -\mu R^* & I-\mu R^{*2} \end{bmatrix} = (\Phi^* \Phi^{*T})^{-1} \qquad \text{(B-9)}$$

The procedure for obtaining rigid body inertia data from (B-9) is to

isolate a 6 × 6 submatrix Φ^* from Φ;

perform the operations indicated on the right hand side of (B-9);

Obtain μ, R* and I in that order from appropriate elements of (B-9).

Note that due to numerical error either in the original data Φ^* or in performing the operations indicated in (B-9), the above procedure is apt to yield ambiguous results. For example, three equations are available for obtaining μ, and in general they will yield values that are somewhat different. Numerical error and ambiguity can be kept to a minimum by using a Φ^* associated with a location close to the mass center so that the μR^* and μR^{*2} terms in (B-9) are small.

Appendix C

Bending Filter Transfer Function Derivation

The bending filters proposed in Reference 5 are in z-transform form:

$$F(z) = \frac{az(z+1)}{(z-b)^3} \tag{C-1}$$

In order to use the filters in the continuous model it is necessary to obtain an* inverse transform of (C-1). Toward this end, expand F(z) in a series of inverse powers of z.

$$F(z) = \frac{a}{z}\left(1+\frac{1}{z}\right)\left(1-\frac{b}{z}\right)^{-3}$$

$$= \frac{a}{2b}\left(1+\frac{1}{z}\right)\sum_{n=1}^{\infty} n(n+1)\left(\frac{b}{z}\right)^n$$

$$= \frac{a}{2b^2}\sum_{n=0}^{\infty} n[(b+1)n+(b-1)]\left(\frac{b}{z}\right)^n \tag{C-2}$$

By definition

$$F(z) = \sum_{n=0}^{\infty} f(nT)z^{-n} \tag{C-3}$$

where T denotes the sampling interval. From (C-2) and (C-3)

$$f(nT) = \frac{an}{2b^2}[(b+1)n+(b-1)]b^n \tag{C-4}$$

---

*Because the z-transform is based on discretely-spaced samples of a time function, the inverse transform is not unique in that it can have any value between sampling points.

To obtain a continuous function of time, take n to be continuous and let n=t/T. Then

$$f(t) = \frac{a}{2b^2T^2}\,[(b+1)t^2+(b-1)Tt]e^{-\beta t} \qquad \text{(C-5)}$$

where

$$\beta = \frac{-\ln b}{T} \qquad \text{(C-6)}$$

The required transfer function is the Laplace transform of the impulsive response (C-5):

$$F(s) = \frac{a}{2b^2T^2}\;\frac{T(b-1)s+[2(b+1)+T\beta(b-1)]}{s^3+3\beta s^2+3\beta^2 s+\beta^3} \qquad \text{(C-7)}$$

REFERENCES

1. Kranton, J., "Stability of the CMG Control System for a Flexible Skylab," Bellcomm Memorandum for File B71 01034, January 28, 1971.

2. "Skylab Subsystem Review Action Item Responses," MSFC, April 1, 1971, pp. (10-44)-(10-55).

3. Gevarter, W. B., "Basic Relations for Control of Flexible Vehicles," AIAA Journal, vol.8, pp.666-672 (April 1970); equation (28).

4. "Revised Vibrational Characteristics of Skylab Orbital Cluster Configurations 1.2 and 3.2 for Control System Design," MSFC Letter S&E-ASTN-ADS-71-8, February 26, 1971; configuration 1.2.

5. Bickle, F. E., "Revised CMG/Vehicle Outer Loop Control Gains and Compensation," Martin Marietta Corporation Inter-Department Communication, February 11, 1971.

6. Zimbleman, H. F., and Jackson, R. S., "ATM PCS (CMG Vehicle and EPC System) Control Gain and Compensation Report," Martin Marietta Technical Report ED-2002-1243, January 19, 1971.

7. Bar-Itzhack, I. Y. and Hou, S. N., "Statistical Analysis of Nonstationary Structural Response Under Feedback Conditions," Bellcomm TM-70-2031-2, April 6, 1970.

8. Smith, P. G., "Numerical Solution of the Matrix Equation $AX+XA^{T}+B=0$," IEEE Trans. Automatic Control, Vol. AC-16, pp. 278-279 (June 1971).

9. Hendricks, T. C. and others, "Crew Motion Data Analysis," Martin Marietta Technical Report ED-2002-644, October 14, 1968.

10. Henize, K. G., letter on the subject: Impact of System Engineering Study "Resolution Accuracy Study for Mirror System on S019 Experiments," dated June 19, 1970, on Experiment S019, Northwestern University, Lindheimer Astronomical Research Center, July 7, 1970.